IMAGE-BASED SIMULATION OF BRAIN ARTERIOVENOUS MALFORMATION HEMODYNAMICS

*Piotr Orlowski, J. Alison Noble, Yiannis Ventikos**

Department of Engineering Science
University of Oxford
Parks Road, Oxford, OX1 3PJ, UK

James Byrne, Paul Summers

Nuffield Department of Surgery
University of Oxford
The John Radcliffe Hospital
Headley Way, Oxford, OX3 9DU, UK

ABSTRACT

A novel image-based patient-specific simulation method has been developed incorporating computational fluid dynamics (CFD) and porous media principles which presents, for the first time, patient-specific blood flow through an arteriovenous malformation of the brain (BAVM). The new approach constructs an image-based geometric model of a malformation where the BAVM nidus is modelled as a porous medium. The method has been applied to a brain BAVM case with two feeding and four draining vessels. A qualitative comparison of the simulation results with blood flow imaging data shows the promise of the approach and suggests that the method may find application in planning for BAVM treatment.

Index Terms— arteriovenous malformation of the brain, computational fluid dynamics, soil mechanics, cardiovascular image analysis, neuro-interventions.

1. INTRODUCTION

A brain AVM (BAVM) is a set of abnormal vessels comprising feeding arteries, draining veins and a collection of arterialized veins called the nidus [1]. Roughly half of BAVMs are treated by embolization of the abnormal vessels. Embolization requires knowledge of the intranidal blood flow in order to plan for the delivery of the emboli material. Clinically, this is often achieved by the acquisition and visualization of an X-ray angiogram sequence or "roadmap".

The main disadvantages of X-ray angiography for this purpose are the low temporal resolution (around 3 frames/sec), the need to acquire data from multiple angles to get a 3D volume of the intranidal flow and invasiveness and it is not quantitative. Thus there is an interest in developing alternative ways to provide this information. This paper addresses these schortcomings by introducing a new, simulation-based, approach.

*PO would like to thank Sloane Robinson LLP for support via a PhD scholarship. PO and YV would like to thank the ESI Group and Dr. M. Megahed for the use of CFD-ACE+.

Prior related research on analysis of blood flow in other abnormal vascular structures, like aneurysms, has used a geometric model reconstruction from a 3D image dataset and simulated flow according to some computational fluid dynamics (CFD) paradigm [2]. However, vessels composing the BAVM nidus are of subvoxel dimension and this makes a full BAVM model analysis, down to microvascular resolution, impossible due to the limited spatial resolution of images. For this reason most recent prior simulation research has concentrated on theoretical modelling of BAVM hemodynamics [3] or statistical analysis of treatment outcomes with respect to adopted intervention strategies [4]. The main contribution of our research is to present, for the first time, a nidus model derived from imagery that is employed for blood flow CFD simulation of a BAVM.

2. METHODS

2.1. BAVM model

The spatial resolution of imaging limits the level of detail that can be extracted around a BAVM. We thus model the BAVM as a two-component model, vessels and a porous "blob" (the nidus). This model is in part motivated by BAVM phantoms used for clinical embolization training that are made out of porous material[5]. The concept naturally extends to an n-component model, where there are n-1 levels of vessels with each level describing vessels in a size range, and a nidus. An example of the BAVM can be seen in Fig. 1.

Consider the nidus component of our model. Transport through porous media can be represented by the momentum conservation equation. body forces are not present and the flow is assumed to be steady, then the governing equation is,

$$\nabla(\epsilon\rho UU) = -\epsilon\nabla p + \nabla(\epsilon\tau) - \frac{\epsilon\mu}{\kappa}U - \frac{\epsilon^3 C_D\rho}{\sqrt{\kappa}}|U|\,U \quad (1)$$

where ρ is the fluid density, p pressure, μ viscosity of the fluid, C_D the quadratic drag factor, τ the shear stress tensor and U

the velocity of the fluid. The permeability κ is the surface area to volume ratio of the porous matrix. The porosity ϵ is defined as the ratio of empty space in a volume to that volume. There are two key parameters governing the physical properties of the modelled BAVM nidus, κ and ϵ parameters that need to be estimated from images for patient-specific modelling. We explain how we do this in the next section.

2.2. Geometry extraction

In our method the extraction of the geometric model of the nidus and of the feeding and draining vessels is based on the manual segmentation of 3D rotational angiography (3DRA) images (used clinically for the visualization of BAVMS). The BAVM 3D volume is segmented into three fields: feeding and draining vessels voxels, nidus voxels and background voxels. Manual segmentation of the vessels is straightforward and is carried up to a few centimeters from the nidus. Feeders and drainers with a radius below three voxels are neglected. All voxels belonging to a volume with a high vascularization density are considered to be part of the nidus. This includes voxels which do not contain vessels but are enclosed within the area. Background voxels are all other voxels. An example of segmentation results is shown in Fig. 2

The vessel and nidus fields are smoothed with an erosion-diffusion filter and are used as the base for the construction of the BAVM surface. The defined volume can then be meshed using a tetrahedral grid which will be used for CFD simulation.

2.3. Porosity model extraction

3D rotational angiography (3DRA) is conventionally used clinically for visualization of the geometry of BAVMs. However, the spatial resolution of 3DRA is relatively low and most inner-nidus voxel intensities result from the mixture of two components: tissue, and contrasted blood. Specifically,

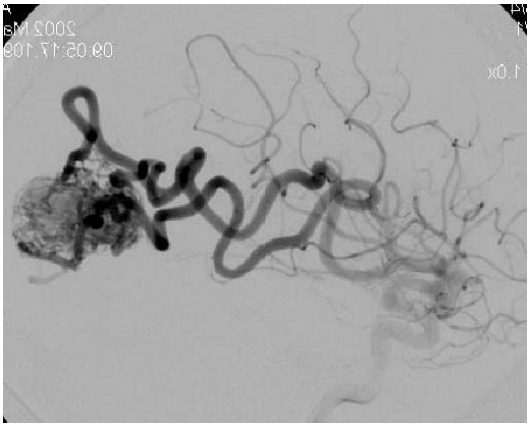

Fig. 1. Example of a 2D BAVM angiogram.

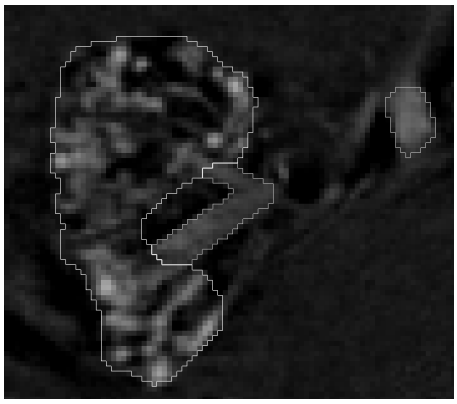

Fig. 2. Slice from a 3DRA BAVM dataset with a segmented nidus and draining vein.

let the intensity I^i of a 3DRA voxel be modelled by a mixture model:

$$I^i = \alpha^i I_1 + (1 - \alpha^i) I_2 \tag{2}$$

where I^i is the value in Hounsfield units of the i^{th} voxel, I_1 is the value of a voxel containing only tissue, I_2 the value of a voxel containing solely contrasted blood and $\alpha^i \in [0, 1]$. The value of I_1 and I_2 can be set based on the value of voxels at the entrance of the nidus and in an area containing noise respectively. The value of porosity ϵ for each voxel can then be defined as:

$$\epsilon^i = \begin{cases} s & I^i < I_1 \\ s + (1 - s)\frac{I^i - I_1}{I_2 - I_1} & I_1 \leq I^i \leq I_2 \\ 1 & I^i > I_2 \end{cases} \tag{3}$$

Where the parameter $s \in [0, 1]$. The setting of this parameter will be discussed in the following section. Let us assume that blood flows through all of the pores (vessels) of the model. Then the permeability of the i^{th} voxel is a function of ϵ. Further, we assume that within a voxel all nidus vessels are straight tubes with the same radius r and with flow governed by Poisseuille's law,

$$Q = \frac{\pi r^4 \Delta p}{8 \mu l}. \tag{4}$$

Here Δp is the pressure gradient in a tube of length l. Then according to Darcy's law,

$$Q = \frac{\kappa d^2 \Delta p}{\mu l} \tag{5}$$

Where d is the length of a side of a uniform voxel, permeability κ can be approximated by

$$\kappa = n \frac{\pi r^4}{8 d^2} \tag{6}$$

Here n is the number of nidus vessels contained in a voxel. Porosity is proportional to n therefore n can be written as

$$\epsilon = n\frac{d\pi r^2}{d^3} \Leftrightarrow n = \epsilon\frac{d^2}{\pi r^2} \tag{7}$$

Combining equations 6 and 7 and taking into account the fact that vessels are not straight cylinders, the permeability can be expressed as

$$\kappa = c\frac{\epsilon r^2}{8\tau} \tag{8}$$

where, as in [6], c was introduced as an empirical geometrical parameter and τ is the tortuosity defined as the square of the ratio of the length of a vessel in a voxel to the length of the voxel's side. In addition, as the radii of the intranidal vessels can vary significantly, the concept of the hydraulic radius $R_h = \frac{\epsilon^3}{a_v(1-\epsilon)^2}$, defined as the ratio of the volume of vessels to the tissue fluid interfacial area, needs to be introduced. a_v is the specific internal surface area, i.e. the ratio of the exposed surface to solid volume). Therefore taking into account the parameter s permeability can be written as

$$\kappa = C_{kc}\frac{(\epsilon - s)^3}{1-\epsilon} \tag{9}$$

Where $C_{kc} = \frac{c}{8a_v^2\tau}$. Permeability has been set to be isotropic for each of the voxels.

3. EXPERIMENTS AND RESULTS

CFD simulation of BAVM haemodynamics requires the following input parameters: (1) nidus porosity and permeability parameters, (2) a geometric model (grid) of the AVM (nidus, and supplying and draining vessels), and (3) simulation boundary conditions. To set the boundary conditions for the simulation problem, blood velocities at the BAVM inlets are extracted from Phase-Contrast Magnetic Resonance PCMRA images of the malformation. The pressure at the outlets is set to 0.

Our model was estimated from images of a BAVM with two feeding arteries and four draining veins. The feeders were supplied from the left basilar artery only. The 3DRA data

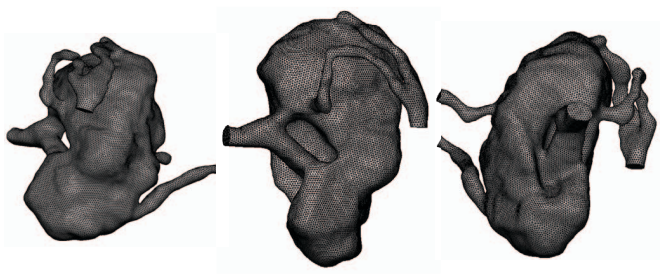

Fig. 3. A mesh of the BAVM with 692,255 cells seen from different angles.

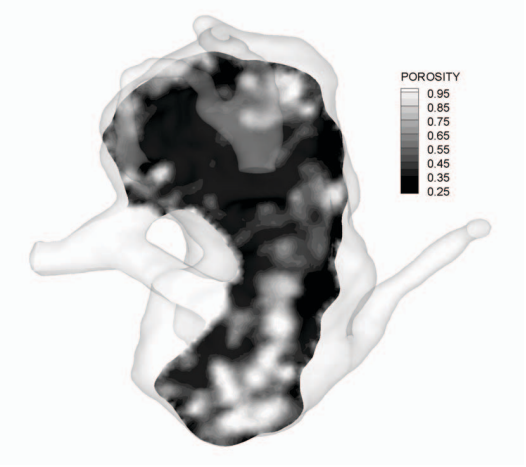

Fig. 4. Porosity field in a slice of the BAVM. $I_1 = -600$, $I_2 = -300$ and $s = 0.2$.

was acquired on a Siemens scanner with image volume size 256x256x230 voxels of spatial resolution 0.578x0.578x0.578 mm. PC-MRA images of the malformation were acquired on GE Medical Systems 1.5T scanner with the following parameters: image size: 256x256x62, in plane resolution: 0.859x0.859 mm slice thickness: 1.2 mm, RT=17 ms, ET=6.2 ms, flip angle: 20°.

The 3DRA dataset was manually segmented. A smoothed surface of the segmented volume was extracted and loaded into GAMBIT a CFD preprocessor from Fluent (ANSYS Inc.) and meshed. The grid consisted of 692,255 cells. Grid independence was assured. A few views of the mesh are given in fig 3. The grid was then exported to CFD-ACE+ (ESI-Group) a CFD simulator. Boundary conditions for the experiment were set based on PC-MRA images of the malformation. Velocity at the inlets was set as the average from their cross-sectional voxels. (velocity being the square root of the sum of squares of corresponding voxel values from the three velocity encoded PC-MRA datasets). Velocities at the inlets 1 and 2 (Fig. 5) were respectively set to 1015 mm/s and 300 mm/s. The drag coefficient C_D was set to 1 (valid for $100 < Re < 10^5$, where Re is the Reynolds number). Porosity and permeability values were set for each cell of the grid according to equations 3 and 9. The I^i value of a cell was the same as the I^i value of the voxel holding the cell's center. Based on the 3DRA dataset I_1 and I_2 were given the values of -600 and -300 respectively. The parameter s was set to 0.2 for numerical reasons and C_{kc} was set to 1000. Cells corresponding to vessel voxels were given a porosity of 1. The resulting porosity field is shown in Fig. 4.

For the purposes of simulation the viscosity of blood was set to $\mu = 0.004kg.m^{-1}.s^{-1}$ and blood density was set to $\rho = 1063kg/m^3$. A second-order accurate finite volume was used. A simulation was run until full convergence. The velocity streamlines in one slice of the BAVM are given in Fig. 6.

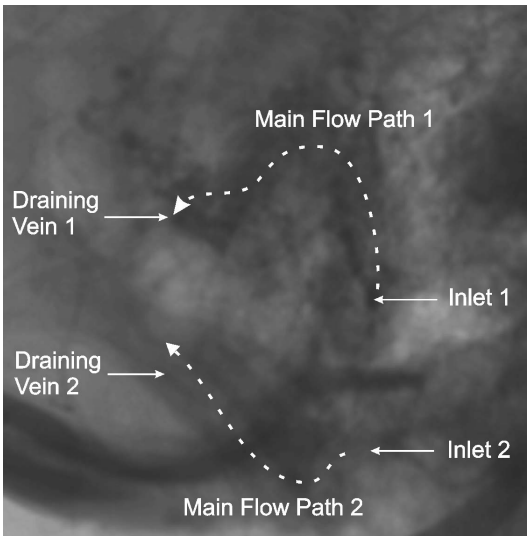

Fig. 5. Digital substraction angiography image of the BAVM showing principal feeding and draining veins as well as the main flow paths within the malformation's nidus.

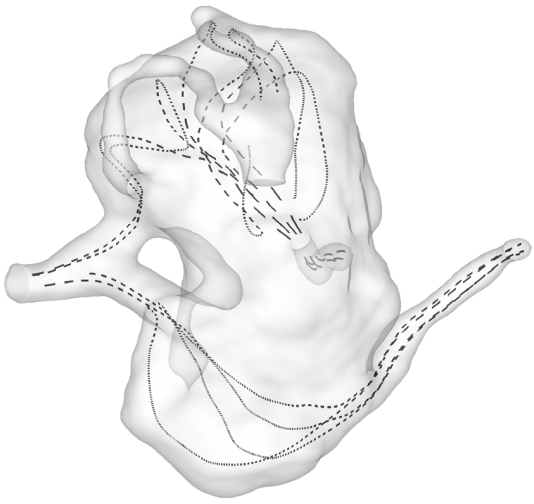

Fig. 6. Simulations results: intranidal velocity streamlines. Thicker line represents a higher velocity magnitude.

The simulation results were compared qualitatively with 2D digital subtraction angiography images of the BAVM. One view is presented in figure 5. The views in figures 5 and 6 are similar. A qualitative comparisons shows that the simulation managed to identify the main flow paths within the AVM. With feeder 1 supplying mainly the upper part of the BAVM and feeder 2 the lower part.

4. DISCUSSION

This work introduced a patient-specific model which enables the use of CFD techniques in the simulation of the BAVMs. Qualitative comparison of simulation results with DSA images was encouraging and suggests that the model could be used in assisting clinicians in BAVM treatment planning. Potential applications include the simulation of the injection of occluding material during embolization. In order to do so the model needs further development. For instance, additional information on the intranidal geometry could be included in the geometry extraction step as the BAVM can often be divided into flow compartments. In addition the influence of the s and C_{kc} parameters on simulation results should be investigated in more detail. Furthermore manual segmentation of the BAVM is time consuming and future work will automate the process. Finally the technique needs to be tested on more BAVM cases and expanded to malformations fed by more than one main artery.

5. REFERENCES

[1] J.V. Byrne, "Cerebrovascular malformations," *European Radiology*, vol. 15, pp. 448–452, 2005.

[2] V.D. Butty, K. Gudjonsson, P Buchel, V.B Makhijani, Yiannis Ventikos, and D. Poulikakos, "Residence times and basins of attraction for a realistic right internal carotid artery with two aneurysms," *Biorheology*, vol. 39, pp. 387–393, 2002.

[3] E. Gao, W.L. Young, G.J. Hademenos, T.F. Massoud, R.R. Sciacca, Q. Ma, S. Joshi, H. Mast, J.P. Mohr, S. Vulliemoz, and J. Pile-Spellman, "Theoretical modelling of arteriovenous malformation rupture risk: a feasibility and validation study," *Medical Engineering and Physics*, vol. 20, pp. 489–501, 1998.

[4] H. Henkes, T.F. Gotwald, S. Brew, F. Kaemmerer, E. Miloslavski, and D. Kuehne, "Pressure measurments in arterial feeders of brain arteriovenous malformations before and after endovascular embolization," *Neuroradiology*, vol. 46, pp. 673–677, 2004.

[5] C.W Kerber, S.T. Hecht, and K. Knox, "Arteriovenous malformation model for training and research," *AJNR Am J Neuroradiol*, vol. 18, pp. 1229–1232, 1997.

[6] Costa Antonio, "Permeability-porosity relationship: A reexamination of the kozeny-carman equation based on a fractal pore-space geometry assumption," *Geophysical Research Letters*, vol. 33, 2006.